

Scaling laws for softened hadron production at LHC energies

D. Rosales Herrera¹, J. R. Alvarado García¹, A. Fernández Téllez¹, E. Cuautle¹,
J. E. Ramírez^{3*}

¹Facultad de Ciencias Físico Matemáticas, Benemérita Universidad Autónoma de Puebla,
Apartado Postal 165, 72000 Puebla, Puebla, Mexico.

²Instituto de Ciencias Nucleares, Universidad Nacional Autónoma de México, Apartado
Postal 70-543, Ciudad de México 04510, México.

³Centro de Agroecología, Instituto de Ciencias, Benemérita Universidad Autónoma de
Puebla, Apartado Postal 165, 72000 Puebla, Puebla, México.

*Corresponding author(s). E-mail(s): jhony.eredi.ramirez.cancino@cern.ch;

Abstract

In this paper, we conduct a data-driven study of the production of softened hadrons and their contribution to the transverse momentum spectrum. To this end, we assume that the production of charged particles at soft and hard scales fundamentally results from the fragmentation of color strings. We analyze the p_T -spectrum data from pp to AA collisions at LHC energies reported by the ALICE Collaboration, finding that, in all cases, the data can be collapsed into a p_T -exponential trend in the range $1 \text{ GeV} < p_T < 6 \text{ GeV}$. With this insight, the description of the p_T -spectrum should contain information on the charged particle production coming from two different sources: fragmentation of color strings and collective phenomena that redistribute the transverse momentum and enhance the production of particles at intermediate p_T . We also found different relations between the effective temperature, multiplicity, and average p_T for pp and AA collisions, indicating inherent dissimilarities between small and large colliding systems. In contrast, the contribution of the softened hadrons to the p_T -spectrum and average p_T collapse onto scaling laws. Our results show that the physical mechanisms producing softened hadrons have similar origins for all colliding systems, revealing a stronger dependence on freeze-out parameters rather than the system size.

1 Introduction

Experimental evidence of the quark-gluon plasma (QGP) formation in heavy ion collision shed light on the properties of the strongly interacting matter under extreme conditions of temperature and pressure [1–4]. The created system efficiently transforms initial spatial anisotropies into correlated momentum disparities among the resultant particles, generating the well-known collective flow [5]. In particular, AA collisions show a radial

flow affecting the p_T -spectrum of produced particles, which is more relevant for heavy hadrons at intermediate p_T as the behavior of the proton-to-pion ratio reveals [6]. Other mechanisms similarly modifying the p_T -spectrum are the suppression of high p_T hadrons, parton recombination, color reconnection, or multiple parton interactions [7–9]. The hydrodynamical model can also explain the flow's origin by assuming a medium's presence [10]. The energy loss due to the parton scattering and bremsstrahlung can suppress the production

of high p_T hadrons [11, 12], leading to the observed jet quenching [13]. These results highlight that a fraction of the produced hadrons at the initial state get softened through the system’s evolution [14].

Similar effects to collective phenomena and radial flow have been observed in events with the largest multiplicities in pp and pPb collisions [15–18], where the softening of high p_T hadrons is less noticeable than in the heavy ion case. Recent discussions about the formation of QGP droplets motivate the search for jet quenching-like effects in small systems [19, 20]. The study of the flow patterns and the strong differences between small and large systems motivates the development of models describing particle production in ultrarelativistic collisions [21]. For instance, the fragmentation of color strings emerging from the colliding partons describes the particle production at the parton level [22]. This phenomenological approach is part of event generators, such as PYTHIA, EPOS, and Herwig, which consider the string fragmentation to describe experimental observables as well as the production of particles at high energies [23]. A fundamental aspect of this framework is incorporating the Schwinger mechanism to describe the p_T -distribution of the charged particles created. The Schwinger mechanism can adequately describe the p_T -spectrum data by considering a stochastic picture of the string tension [24, 25]. In particular, it is possible to reproduce the asymptotic behaviors experimentally observed by assuming a heavy-tailed description for the string tension fluctuations [25–28]. An immediate consequence of this approach is that the systems formed in ultrarelativistic collisions are no longer thermal, emerging nonequilibrium temperature fluctuations along the systems [28]. Nevertheless, for high multiplicity events, the aforementioned collective phenomena redistribute the p_T of a portion of the produced hadrons, enhancing the p_T -spectrum at intermediate values (1–6 GeV). In this way, the fragmentation of color strings fails to capture the softened hadron production.

This paper aims to describe the entire p_T -spectrum of charged particles produced in ultrarelativistic collisions. In particular, we are interested in identifying the softened hadron production and quantifying their contribution to the freeze-out parameters. To this end, we analyze the experimental p_T -spectrum data at intermediate

p_T values by assuming a color string fragmentation baseline for charged particle production. This procedure allows us to data-driven infer the functional form of the softened hadron contribution to the p_T -spectrum, which is now compounded by the sum of the particle production coming from string fragmentation and softened hadrons. Then, we can determine the contribution of the softened hadrons to the freeze-out parameter, finding scaling laws in terms of the multiplicity rather than the system’s size.

The rest of the manuscript is organized as follows. In Sec. 2, we use a nonextensive string fragmentation framework to describe the p_T spectrum of the charged particles produced in high-energy collisions. This approach correctly reproduces the asymptotic behaviors experimentally observed. We use this approach as a baseline for the particle production at the soft and hard scales. In Sec. 3, we data-driven infer that softened hadrons mainly contribute to the p_T -spectrum at the intermediate region, following an exponential decay independently of the system’s size, center of mass energies, or event classifications. Consequently, the softened particles are produced at a higher temperature than the soft scale. With this insight, in Sec. 4, we describe the entire p_T spectrum by considering that the charged particle production comes from combining the color string fragmentation and collective phenomena. The latter redistributes the p_T of a fraction of particles, leading to the softened hadrons. In Sec. 5, we quantify the contribution of the softened hadrons to the p_T -spectrum, the multiplicity, and $\langle p_T \rangle$, finding scaling laws as function of the the freeze-out parameters. Finally, we present our final remarks and conclusions in Sec. 6.

2 p_T -spectrum from a nonextensive description

String models describe particle production by the fragmentation of color strings emerging from the colliding partons. The particle-antiparticle creation process involves the Schwinger mechanism, given by [29]

$$\frac{dN}{dp_T^2} \sim e^{-\pi p_T^2/x^2}, \quad (1)$$

which is the p_T -distribution when the charged particles are created from the fragmentation of color

strings with tension x^2 . In a general scenario the string tension may fluctuate accordingly to a probability density function $P(x)$ [24, 25]. Then, the p_T -spectrum must be computed as the convolution

$$\frac{dN}{dp_T^2} \sim \int_0^\infty e^{-\pi p_T^2/x^2} P(x) dx. \quad (2)$$

For instance, the well-known thermal distribution

$$\frac{dN}{dp_T^2} \sim e^{-p_T/T_{\text{th}}},$$

with soft scale $T_{\text{th}} = \langle p_T^2 \rangle / 2$, is obtained by considering Gaussian string tension fluctuations [24, 25]. This approach can describe the experimental data at very low energy collisions or low p_T values. However, it fails to describe the case of high energy collisions at high p_T values. In part, it is because of the probability of hard gluon emission from strings growing with the center of mass energy, as stated in the Lund model [22], resulting in additional string tension fluctuations that the Gaussian distribution can no longer describe.

To incorporate the hard part of the p_T -spectrum, we must raise the probability of observing strings with higher tension. This can be achieved by enhancing the tail of the Gaussian distribution by promoting it to a q -Gaussian distribution

$$P(x) = \mathcal{N}_q \left[1 + (q-1)x^2/2\sigma^2 \right]^{\frac{1}{1-q}}, \quad (3)$$

which is a heavy-tailed probability density function broadly used to study nonequilibrium systems [30]. In Eq. (3), \mathcal{N}_q is the normalization constant, q is the deformation parameter quantifying the deviations from the Gaussian behavior, and σ is related to the width of the distribution [30]. In this context, q must take a value between 1 and 3 to guarantee the convergence of the normalization constant and allow variations in the string tension across the range from zero to infinity [27, 30, 31].

In this manner, by assuming a q -Gaussian description of the string tension fluctuations, the p_T -spectrum becomes a Tricomi's function

$$\frac{dN}{dp_T^2} \sim U(a, 1/2, z_0 p_T^2), \quad (4)$$

with $a = 1/(q-1) - 1/2$ and $z_0 = \pi(q-1)/2\sigma^2$. Interestingly, this U function has the experimentally observed asymptotic behaviors. At low p_T values, U behaves as the thermal distribution, i.e., $U \sim e^{-p_T/T_U}$ with soft scale $T_U = B(a, 1/2)/\sqrt{4\pi z_0}$, and B being the beta function [26]. Conversely, it behaves as the power law $U \propto (p_T^2)^{\frac{1}{2} - \frac{1}{q-1}}$ for high p_T values. In particular, this function adequately fits the p_T -spectrum data of the charged particle and Higgs boson production in pp collisions [25–28]. This is corroborated by analyzing the experimental data of minimum bias and low multiplicity events in pp collisions and peripheral events in AA collisions reported by ALICE Collaboration (see top panels of Fig. 1) [32–36]. One advantage of this approach is that the U function controls the uncertainty propagation in all cases. Additionally, the fit to data ratio remains close to 1 for all the analyzed cases (see bottom panels of Fig. 1).

However, the U function deviates from the p_T -spectrum data for the most central heavy ion collisions at intermediate p_T values. In fact, these effects are more noticeable for high multiplicity events [27]. It may occur because of an excess of charged hadrons detected with p_T approximately from 1 to 6 GeV, usually explained by mechanisms beyond the string fragmentation, such as experimentally measured signals in AA collisions as well as similar signals modeled and observed in high multiplicity events in pp collisions [9, 20]. In this sense, we distinguish two contributions to the p_T -spectrum to describe the experimental data. The first assumes the production of charged particles through the fragmentation of color strings, described by the Tricomi's function [25–27]. The second part considers softened hadrons acquiring their transverse momentum through processes beyond string fragmentation, enhancing the p_T -spectrum at intermediate p_T values.

We must emphasize that dN/dp_T^2 denotes the yield of charged particles normalized by $2\pi p_T$, the number of events, and pseudorapidity interval. Nevertheless, some experiments report the spectrum without the p_T normalization, usually denoted by dN/dp_T . In such cases, Eq. (4), and the following presented in this manuscript, must be multiplied by p_T to fit the data correctly, keeping all the results discussed in this paper valid.

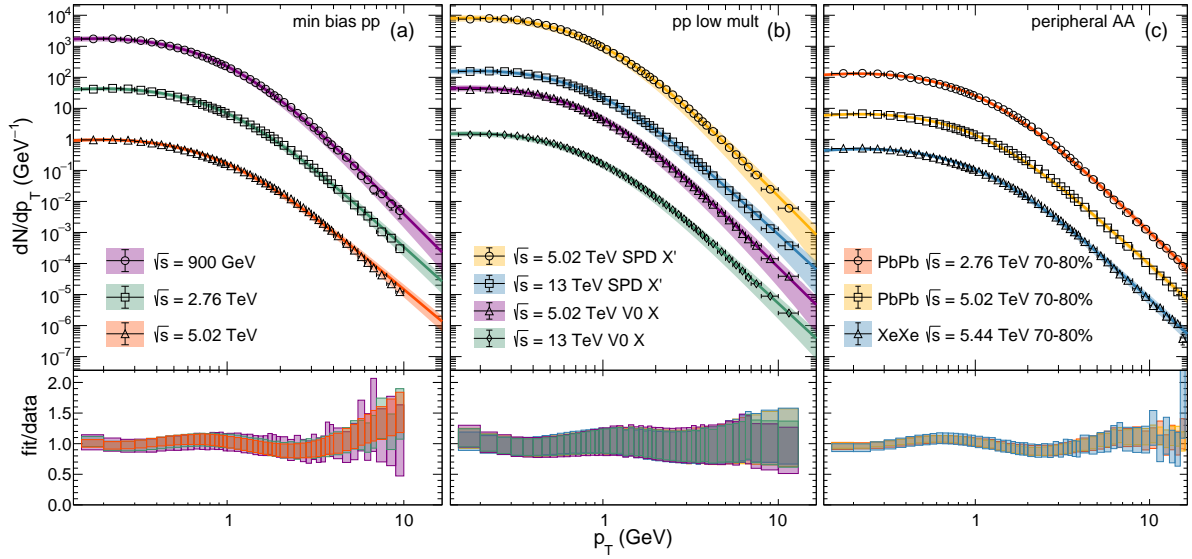


Fig. 1 Experimental data of minimum bias (a), and low multiplicity events (b) in pp collisions, and peripheral events (c) in AA collisions at different center of mass energies reported by the ALICE Collaboration accurately described by the Tricomi's function (4).

3 Elucidating the softened hadron production

We assess the contribution of softened hadrons by analyzing the experimental data of pp, AA, and pPb collisions at different center of mass energies, centralities, and multiplicity classifications. To this end, we assume that the contributions of soft and hard scales mainly come from the string fragmentation picture. As a first step, we search for the best fit of the U function (4) to data by excluding the intermediate p_T region. Therefore, we interpolate the yield produced by the string fragmentation (Y_{sf}) in the intermediate region by evaluating the bin centers onto the $p_T U$ function. We found that the difference of the experimental yield data (Y_{data}) and Y_{sf} behaves as $Y_{data} - Y_{sf} = a_{th} p_T e^{-p_T/t_{th}}$ in the range of 1 to 6 GeV for all data sets analyzed in this manuscript. In Fig. 2, we plot $(Y_{data} - Y_{sf})$ normalized by $a_{th} t_{th}$ as a function of the transverse momentum scaled by t_{th} . Note that we use Y to denote the yield dN/dp_T to improve notation. Remarkably, all the analyzed data at intermediate p_T values collapse following a universal behavior. We must emphasize that this fact does not imply that the production of softened hadrons comes from thermal processes, but these particles redistribute their transverse momentum in this form.

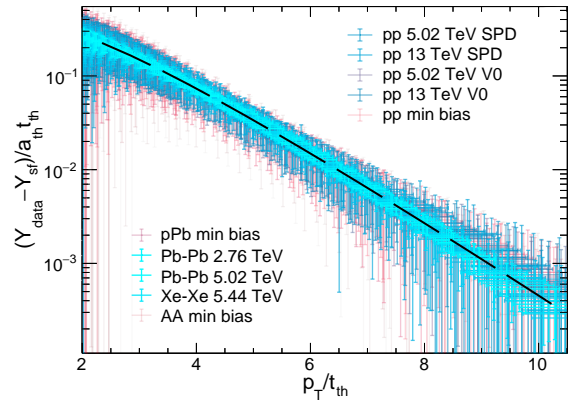


Fig. 2 Difference of experimental yield data (Y_{data}) and the interpolated yield (Y_{sf}) normalized by $a_{th} t_{th}$ as a function of p_T/t_{th} for all the experimental analyzed data at intermediate p_T region. Error bars are the uncertainty propagation of the experimental data together with the fitting parameter errors. The dashed line corresponds to the function $x e^{-x}$.

4 Description of the complete p_T -spectrum

Supported by the previous result on the soft hadron production discussed in Sec. 3, we propose to add a p_T -exponential term in Eq. (4) to obtain

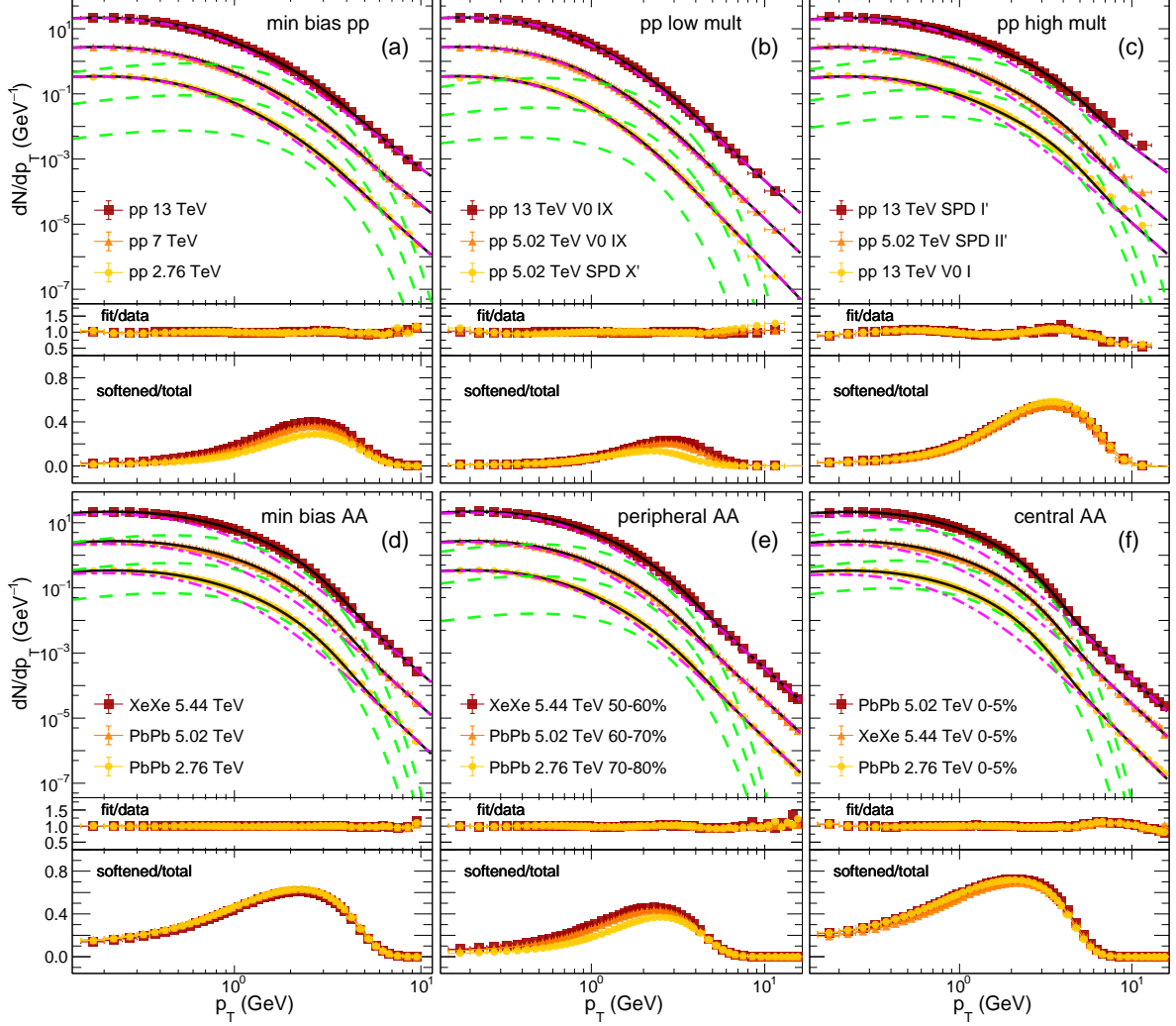


Fig. 3 Sample of the dN/dp_T data sets analyzed for pp collision: (a) minimum bias, (b) low multiplicities, and (c) high multiplicities. For PbPb and XeXe collisions: (d) minimum bias, (e) peripheral, and (f) central. The fit to data and softened hadrons' contribution to total charged particle production ratios are plotted for each case. The dN/dp_T data sets are plotted with marks. Solid lines correspond to the total fit (5). Dash-dotted and dashed lines are the Tricomi's function and p_T -exponential contributions to the total charged particle production, respectively. We scaled all data sets to improve visualization.

a complete description of the p_T -spectrum, i.e.,

$$\frac{dN}{dp_T^2} = A_U U(a, 1/2, z_0 p_T^2) + A_{th} e^{-p_T/T_{th}}, \quad (5)$$

where T_{th} corresponds to the p_T scale related to the softened hadron production. We fit Eq. (5) to the p_T -spectrum data at midrapidity reported in Refs. [33–36] by the ALICE Collaboration for pp, pPb, XeXe, and PbPb collisions at LHC energies considering V0, SPD, and centrality classifications. In Eq. (5), the free parameters A_U and A_{th}

can be understood as the weights for the contribution of the particles produced by the string fragmentation and softened hadrons to the total yield, respectively.

In Fig. 3, we show samples of fits of Eq. (5) to dN/dp_T data sets of pp collisions [(a) minimum bias, (b) low and (c) high multiplicity events], and AA collisions [(d) minimum bias, (e) peripheral and (f) central events]. In all cases, we show the contribution fraction to the total yield of the functions $p_T U$ (pink dash-dotted line) and $p_T e^{-p_T/T_{th}}$

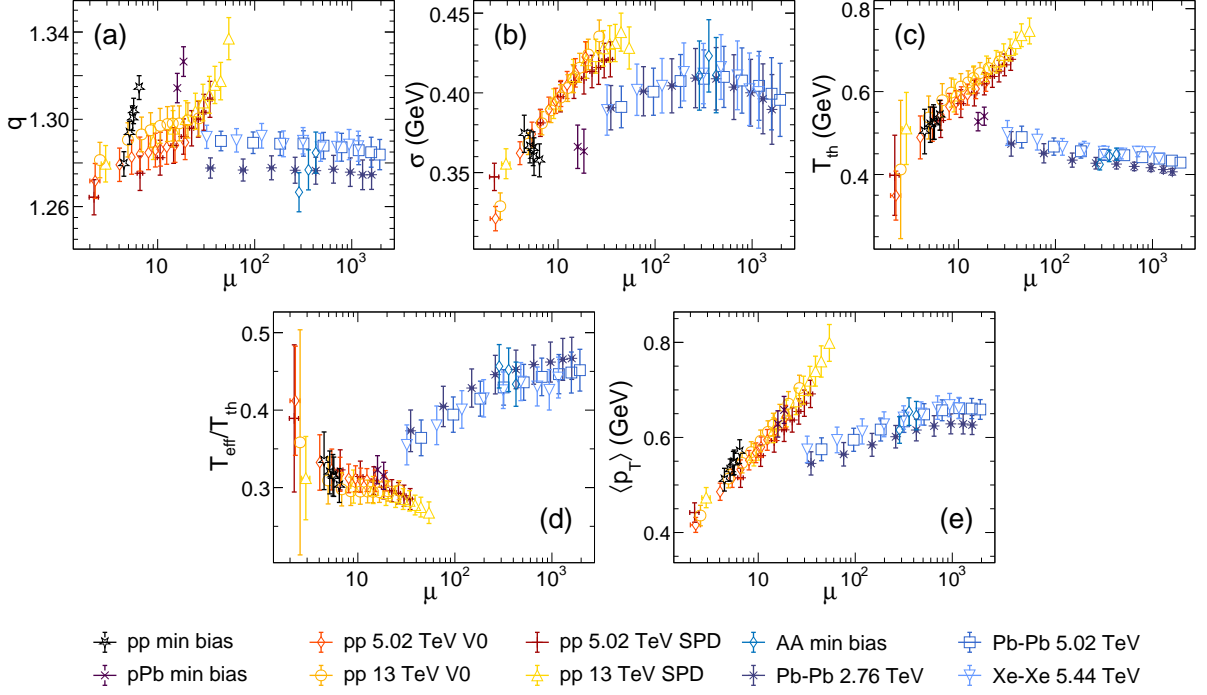


Fig. 4 Multiplicity (μ) dependence of the fitting parameters (a) q , (b) σ , (c) T_{th} , (d) the T_{eff}/T_{th} ratio, and (e) $\langle p_T \rangle$ for all analyzed data.

(green dashed line). In particular, the highest values of the ratio of softened hadrons contribution to total yield indicate the p_T bins wherein the softened hadrons become relevant, which occurs at the intermediate p_T region. Additionally, we found that $\chi^2/\text{nfd} < 1$ for all the analyzed data.

On the other hand, Figures 4 (a)-(c) show the value of the fitting parameters q , σ , and T_{th} as a function of the multiplicity for the data sets analyzed, respectively. These parameters allow us to characterize the properties of the systems through the p_T -spectrum. For instance, in the limit of low p_T , Eq. (5) resembles the thermal distribution with effective temperature:

$$T_{eff}^{-1} = \frac{1}{A_U^* + A_{th}} \left(\frac{A_U^*}{T_U} + \frac{A_{th}}{T_{th}} \right), \quad (6)$$

where $A_U^* = \sqrt{\pi} A_U / \Gamma(a+1/2)$. The effective temperature T_{eff} can be understood as the soft scale linked to the complete p_T -spectrum, considering the contribution of charged particle production coming from string fragmentation and collective phenomena. This is computed over the ensemble of collision events occurring under the same biases [27]. Notice that the definition of T_{eff} in Eq. (6)

is valid for all systems and it is computed by using the fitting parameters extracted from analyzing the p_T -spectrum. We expect that T_{eff} will exhibit some system-size dependence because the p_T -spectrum behaves and evolves differently with multiplicity for pp and AA collisions. However, in all cases, we found that $T_{eff} < T_{th}$ (see Fig. 4 (d)). It means that the softened hadrons take p_T values beyond the soft scale and enhance the spectrum at the intermediate p_T region, which happens at larger p_T values for pp than heavy ion collisions. This is a consequence of the larger values of T_{th} for pp than AA (see Fig. 4 (c)). The shift of the p_T scale where the softened hadrons' contribution takes its maximum values in pp and AA collisions is consistent with the system's size effects, as shown in the ratio of the softened hadrons' contribution to the total charged particle production plotted in Fig. 3.

Another interesting asymptotic limit occurs at high- p_T values. In this limit, Eq. (5) behaves as the power law $(p_T^2)^{\frac{1}{2} - \frac{1}{q-1}}$ because the contribution of the p_T -exponential term vanishes in this limit. Notice that the relevance of q lies in describing the shape of the p_T -spectrum tail. Lower q values

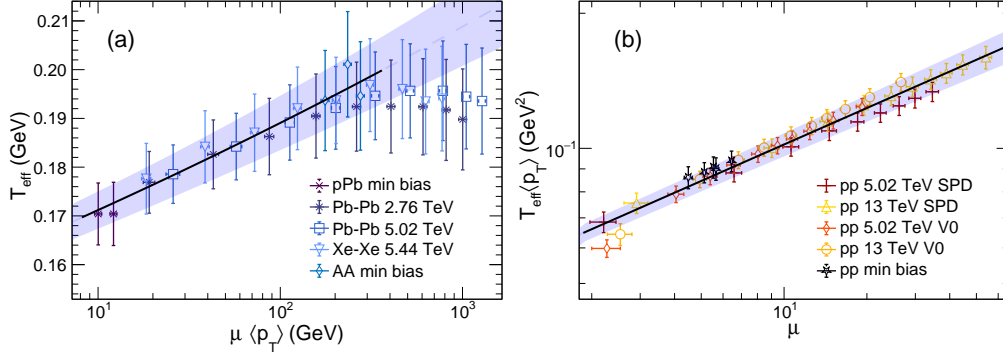


Fig. 5 (a) Effective temperature as a function of $\mu\langle p_T \rangle$ for pPb and AA collisions systems, where μ denotes the multiplicity. The dashed line corresponds to the extrapolation of the data trend for $\mu\langle p_T \rangle > 300$ GeV. (b) $T_{\text{eff}}\langle p_T \rangle$ as a function of the multiplicity (μ) for pp collisions. Shaded regions correspond to the $2\text{-}\sigma$ uncertainty propagation.

mean a decrement in the probability of producing high p_T hadrons. In fact, for AA collision, we found a saturation on q , and it slightly decreases at the largest multiplicity classes (see Fig. 4 (a)), meaning the suppression of the high- p_T particle production in the most central collisions. This effect is aligned with the jet-quenching phenomena reported in heavy ion collisions. In these large systems, this behavior is related to the energy loss, which mainly affects partons originated from deep scattering processes, resulting in a suppression of high- p_T hadrons [37–39]. Conversely, in pp collisions, the suppression of high-momentum hadrons is expected to be lesser due to the system size. Notice that our findings of the contribution of the softened hadrons agree with those observations.

In addition, the computation of the average p_T from the p_T -spectrum must take into account the extra p_T from the phase space factor, i.e.,

$$\langle p_T \rangle = \frac{\int_0^\infty p_T^2 \frac{dN}{dp_T^2} dp_T}{\int_0^\infty p_T \frac{dN}{dp_T^2} dp_T}. \quad (7)$$

Then, for the p_T -distribution given by (5), we found

$$\langle p_T \rangle = \frac{A_U I_1 \langle p_T \rangle_U + 2A_{\text{th}} T_{\text{th}}^3}{A_U I_1 + A_{\text{th}} T_{\text{th}}^2}, \quad (8)$$

where

$$I_1 = \int_0^\infty p_T U dp_T, \\ A_U I_1 = A_U^* \sigma^2 / \pi (5 - 3q),$$

and

$$\langle p_T \rangle_U = \sigma \sqrt{2} \Gamma(a - 3/2) / \sqrt{\pi(q - 1)} \Gamma(a - 1),$$

which converges if $1 < q < 3/2$ [25]. Notice that we have computed the average p_T by integrating over $[0, \infty)$. Figure 4 (e) contains our results of the $\langle p_T \rangle$ calculations. However, we reproduce the values of $\langle p_T \rangle$ by numerically integrating over the p_T range set up by the ALICE Collaboration reported in Ref. [36].

We found that the effective temperature shows different behaviors in small and large systems. For instance, T_{eff} scales as $(\mu\langle p_T \rangle)^{\beta_1}$ in the cases of AA and pPb collisions, where $\beta_1 = 0.043(2)$ and μ denotes the average multiplicity of charged particles per pseudorapidity interval. The factor $\mu\langle p_T \rangle$ is relevant because it is related to the Bjorken energy [40], which can now be rewritten only in terms of the effective temperature. Notice that we are referring to Bjorken energy instead of the Bjorken energy density. The latter needs to be divided by the transverse area and proper time. Conversely, as the multiplicity increases, T_{eff} saturates for $\mu\langle p_T \rangle > 300$ GeV (see Fig 5 (a)), also observed in other analyses of experimental data [41, 42]. On the other hand, for pp collisions, we found that the effective temperature relates to multiplicity and $\langle p_T \rangle$ through $T_{\text{eff}} \propto \mu^{\beta_2} / \langle p_T \rangle$, with $\beta_2 = 0.270(9)$, as shown in Fig. 5 (b). We must emphasize that our findings reveal two distinct behaviors of the effective temperature depending on the kind of the analyzed system. These behaviors are solid evidence of the differences between the systems formed in small and large collisions and their posterior evolution.

5 Softened hadrons' contribution to the p_T -spectrum, N_{ch} and $\langle p_T \rangle$

To quantify the contribution of the softened hadrons to the physical observables computed from the p_T -spectrum, we define

$$E_n = \frac{A_{\text{th}} \int_0^\infty p_T^n e^{-p_T/T_{\text{th}}} dp_T}{\int_0^\infty p_T^n \frac{dN}{dp_T^2} dp_T} = \frac{A_{\text{th}} n! T^{n+1}}{A_U I_n + A_{\text{th}} n! T^{n+1}}, \quad (9)$$

where $I_n = \int_0^\infty p_T^n U dp_T$ is well defined if $q < (4+n)/(2+n)$ [25].

In particular, the cases $n = 0, 1, 2$ correspond to the weighted contribution of softened hadrons to the p_T -spectrum, number of charged particles produced (N_{ch}), and $\langle p_T \rangle$, respectively. Note that for p_T -spectra with no softened hadron production $E_n = 0$, indicating all the particle production comes from the fragmentation of color strings. However, as the mechanisms beyond the string fragmentation appear, the hadrons' p_T is redistributed in a particular way that increases the E_n values.

The contribution of the softened hadrons to the p_T -spectrum is quantified by Eq. (9) for $n = 0$, denoted by E_{dN/dp_T^2} . We found that $E_{dN/dp_T^2} \propto (\mu \langle p_T \rangle)^{\beta_3}$, with $\beta_3 = 0.43(1)$ (see Fig. 6 (a)). Interestingly, this relation stands for the p_T -spectrum data from pp to AA collisions, indicating that the production of hadrons with intermediate p_T increases with the midrapidity Bjorken energy [40, 41].

The fraction of the total yield composed by the softened hadrons is computed using Eq. (9) for $n = 1$, denoted by $E_{N_{\text{ch}}}$. Figure 6 (b) shows the behavior of $E_{N_{\text{ch}}}/\langle p_T \rangle^2$ as a function of multiplicity. We found that this ratio scales for all the analyzed data as μ^{β_4} , with $\beta_4 = 0.08(1)$. Notice that $E_{N_{\text{ch}}}$ vanishes for the lowest multiplicity events. In fact, in the lowest multiplicity classes of pp collisions, our results indicate that the softened hadron production is, on average, one particle per 50 events, which assures that the production of charged hadrons is due to the fragmentation of color strings in this limit. This means the probability of producing this kind of particle is very low but grows with multiplicity. For comparison, the softened hadron production for the lowest multiplicity events in pp collisions at 13 TeV is

two orders of magnitude lower than for the cases of the highest multiplicity classes. Interestingly, the cases of the highest multiplicity pp collisions have comparable values of the fraction of the total yield of peripheral AA collisions. Moreover, for the most central AA collisions, $E_{N_{\text{ch}}}$ takes its maximum value, and the total yield is composed of around 30% of softened hadrons.

The softened hadrons' contribution to $\langle p_T \rangle$ is given by Eq. (9) for $n = 2$, denoted by $E_{\langle p_T \rangle}$. In Fig. 6 (c), we plot the ratio $E_{\langle p_T \rangle}/\langle p_T \rangle$ as a function of the multiplicity, which collapses following a monotone increasing trend for all the analyzed cases. Interestingly, the data of the ratio $E_{\langle p_T \rangle}/\langle p_T \rangle$ can be well described by the scaling relation $E_{\langle p_T \rangle}/\langle p_T \rangle \propto \mu^{\beta_5} + e^{-2/\mu} - 1$, with $\beta_5 = 0.20(1)$. The latter has two asymptotic behaviors. In the case of $\mu \rightarrow 1$, we found $E_{\langle p_T \rangle}/\langle p_T \rangle \propto \ln \mu$. On the other hand, for events with high multiplicity, $E_{\langle p_T \rangle}/\langle p_T \rangle \propto \mu^{\beta_5}$. Even though we have found a universal scaling law that includes the data of pp, pPb, and AA collisions, the two distinct asymptotic behaviors may indicate size effects for small and large systems in producing the softened hadrons. In particular, the large production of softened hadrons for the highest multiplicity events in AA collisions leads to a saturation and a possible reduction of the average p_T (see Fig. 4 (e)) [36], which is consistent with large effects from collective phenomena that degrade the p_T of the hard hadrons, which later produce particles at a lower p_T .

To close this section, let us comment on the results associated with the minimum bias cases, whose results set them apart as outliers. This may happen since the minimum bias data contains the total information from all the multiplicity classes. Although high multiplicity events drive the shape of the p_T spectrum tail and enhance the production of softened hadrons, their contributions to the freeze-out parameters are lower than those provided by the low multiplicity events.

6 Conclusions

In summary, we described the experimental p_T -spectrum data through Tricomi's function by assuming that the fragmentation of color strings is a baseline for the charged particle production. However, this approach deviates from data at intermediate p_T region in the cases of the

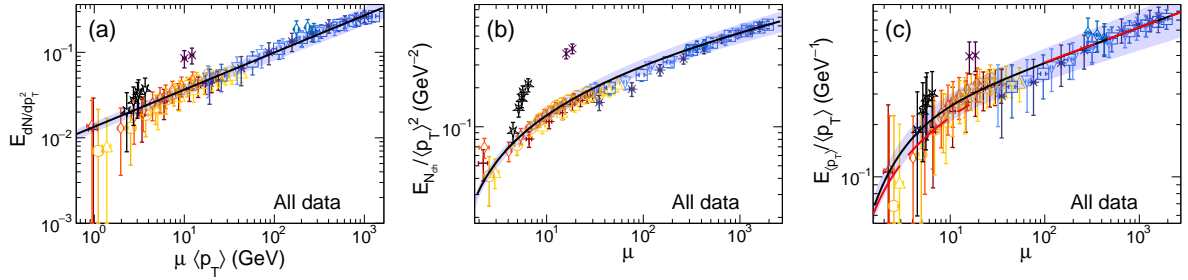


Fig. 6 (a) Softened hadrons contribution to the p_T -spectrum as a function of $\mu\langle p_T \rangle$ for all the analyzed cases. (b) The fraction of the total yield composed by the softened hadrons as a function of the multiplicity. (c) Dependence of $E_{\langle p_T \rangle}/\langle p_T \rangle$ on the multiplicity for all the analyzed cases. The dashed lines show the asymptotic behaviors of the scaling law at low and high multiplicities. In all panels, solid lines correspond to the scaling laws. Shaded regions correspond to the $2\text{-}\sigma$ uncertainty propagation.

most energetic collisions, highest multiplicities, and central AA collisions. We assumed that such deviation is originated by the production of softened hadrons coming from processes beyond string fragmentation, such as color reconnection, parton recombination, jet quenching, energy loss, and flow, among other collective phenomena. Through a data-driven study, we found that such deviations follow a universal behavior that collapses into a p_T -exponential decay in a range of 1 GeV to 6 GeV, which stands for the experimental data of pp, pPb, PbPb, and XeXe collisions at LHC energies. Supported by this insight, we describe the entire p_T -spectrum of charged particle production by incorporating a p_T -exponential term to the Tricomi's function (see Eq. (5)). Then, we analyzed the p_T -spectrum data reported by the ALICE Collaboration concerning the production of charged particles in ultrarelativistic collisions from pp to AA, considering different biases, namely minimum bias, multiplicity, and centrality classifications [33–36]. Remarkably, Eq. (5) accurately describes the p_T -spectrum data for all the analyzed cases. We recall that the Tricomi's function is deduced from a nonextensive description of the string tension fluctuations, which is inherited by Eq. (5). Thus, it preserves the power law tail behavior in the limit of high p_T values. Note that the additional p_T -exponential enhances the soft part, reaching its maximum contribution at intermediate p_T but vanishes at high p_T . In fact, the inverse effective temperature is computed as a weighted sum of T_U^{-1} and T_{th}^{-1} . We must emphasize that the p_T -exponential term in Eq. (5) does not mean that thermal processes

produce the softened hadrons. However, the aforementioned mechanisms redistribute the transverse momentum in this particular way.

We found an enhancement of the p_T -spectrum for intermediate p_T values, which is more noticeable as the multiplicity increases (see Fig. 3). It is consistent with similar signals for QGP formation reported by other analyses, such as the two particle angular correlations and collective flow effects [16, 43]. In the cases of heavy ion collision, we observed that the maximum contribution of the softened hadrons to the p_T -spectrum occurs for p_T values below than the case of pp collisions. This difference is expected because of the system's size effects: the larger the systems are, the more relevant suppression of high p_T hadrons.

Another evidence of the system's size effects is observed in the effective temperature, which behaves differently for small and large systems. In pp collisions, the combination $T_{eff}\langle p_T \rangle$ data collapses onto a power law trend with variable μ . In the cases of pPb and AA collisions, T_{eff} grows as a power law in the variable $\mu\langle p_T \rangle$, which occurs for $\mu < 600$ or $\mu\langle p_T \rangle < 300$ GeV, saturating for larger μ values. Note that $\mu\langle p_T \rangle$ is proportional to the Bjorken energy, which now can be rewritten in terms only of the effective temperature.

We also found that the contribution of the softened hadrons to the p_T -spectrum and $\langle p_T \rangle$ can collapse in global trends. It is worth mentioning that our results indicate a close relation between E_{dN/dp_T^2} and the Bjorken energy. Moreover, the ratio $E_{\langle p_T \rangle}/\langle p_T \rangle$ as well as $E_{N_{ch}}/\langle p_T \rangle^2$ only depend on the multiplicity. Our results on

E_{dN/dp_T^2} and $E_{\langle p_T \rangle}$ are consistent with other analyses claiming collective effects in both pp and AA collisions [44, 45].

The model presented in this manuscript is helpful for quantifying the fraction of softened hadrons with intermediate p_T values and their contribution to the p_T -spectrum, effective temperature, and $\langle p_T \rangle$. The main results presented in this manuscript are the scaling laws for the contribution of the softened hadrons to the p_T -spectrum and average p_T . From this, we can conclude that the physical mechanisms producing the charged softened hadrons have similar origins for all colliding systems. However, the approach presented here cannot distinguish the mechanisms for producing the softened hadrons. Nevertheless, by using our methodology, it is possible to estimate the composition of the softened hadrons by computing $E_{N_{ch}}$ for the yield of identified particles. Additionally, our results can be helpful in improving color string based models and computational tools used to simulate high energy collisions.

Acknowledgments

This work was funded by Consejo Nacional de Humanidades, Ciencias y Tecnologías (CONAHCYT-México) under the project CF-2019/2042, graduated fellowship grant number 1140160, and postdoctoral fellowship grant numbers 645654 and 289198, and DGAPA-PAPIIT BG100322 project.

References

- [1] BRAHMS Collaboration: Quark–gluon plasma and color glass condensate at RHIC? The perspective from the BRAHMS experiment. Nucl. Phys. A **757**(1), 1–27 (2005) <https://doi.org/10.1016/j.nuclphysa.2005.02.130>
- [2] PHOBOS Collaboration: The PHOBOS perspective on discoveries at RHIC. Nucl. Phys. A **757**(1), 28–101 (2005) <https://doi.org/10.1016/j.nuclphysa.2005.03.084>
- [3] STAR Collaboration: Experimental and theoretical challenges in the search for the quark–gluon plasma: The STAR Collaboration’s critical assessment of the evidence from RHIC collisions. Nucl. Phys. A **757**(1), 102–183 (2005) <https://doi.org/10.1016/j.nuclphysa.2005.03.085>
- [4] PHENIX Collaboration: Formation of dense partonic matter in relativistic nucleus–nucleus collisions at RHIC: Experimental evaluation by the PHENIX Collaboration. Nucl. Phys. A **757**(1), 184–283 (2005) <https://doi.org/10.1016/j.nuclphysa.2005.03.086>
- [5] Polleri, A., Bondorf, J.P., Mishustin, I.N.: Effects of collective expansion on light cluster spectra in relativistic heavy ion collisions. Physics Letters B **419**(1), 19–24 (1998) [https://doi.org/10.1016/S0370-2693\(97\)01455-X](https://doi.org/10.1016/S0370-2693(97)01455-X)
- [6] ALICE Collaboration: Production of charged pions, kaons, and (anti-)protons in pb-pb and inelastic pp collisions at $\sqrt{s_{NN}} = 5.02$ tev. Phys. Rev. C **101**, 044907 (2020) <https://doi.org/10.1103/PhysRevC.101.044907>
- [7] Das, K.P., Hwa, R.C.: Quark-antiquark recombination in the fragmentation region. Phys. Lett. B **68**(5), 459–462 (1977) [https://doi.org/10.1016/0370-2693\(77\)90469-5](https://doi.org/10.1016/0370-2693(77)90469-5)
- [8] Hwa, R.C., Yang, C.B.: Recombination of shower partons in fragmentation processes. Phys. Rev. C **70**, 024904 (2004) <https://doi.org/10.1103/PhysRevC.70.024904>
- [9] Cuautle, E., Ortiz, A., Paic, G.: Effects produced by multi-parton interactions and color reconnection in small systems. Nucl. Phys. A **956**, 749–752 (2016) <https://doi.org/10.1016/j.nuclphysa.2016.02.031>
- [10] Belenkij, S.Z., Landau, L.D.: Hydrodynamic theory of multiple production of particles. Usp. Fiz. Nauk **56**, 309 (1955) <https://doi.org/10.1007/BF02745507>
- [11] Baier, R., Schiff, D., Zakharov, B.G.: Energy loss in perturbative QCD. Ann. Rev. Nucl. Part. Sci. **50**, 37–69 (2000) <https://doi.org/10.1146/annurev.nucl.50.1.37>

- [12] Zakharov, B.G.: Parton energy loss in an expanding quark-gluon plasma: Radiative versus collisional. *JETP Lett.* **86**, 444–450 (2007) <https://doi.org/10.1134/S0021364007190034>
- [13] CMS Collaboration: Observation and studies of jet quenching in PbPb collisions at nucleon-nucleon center-of-mass energy = 2.76 TeV. *Phys. Rev. C* **84**, 024906 (2011) <https://doi.org/10.1103/PhysRevC.84.024906>
- [14] PHENIX Collaboration: High p_T charged hadron suppression in Au + Au collisions at $\sqrt{s_{NN}} = 200$ GeV. *Phys. Rev. C* **69**, 034910 (2004) <https://doi.org/10.1103/PhysRevC.69.034910>
- [15] ALICE Collaboration: Multiplicity dependence of pion, kaon, proton and lambda production in p-Pb Collisions at $\sqrt{s_{NN}} = 5.02$ TeV. *Phys. Lett. B* **728**, 25–38 (2014) <https://doi.org/10.1016/j.physletb.2013.11.020>
- [16] CMS Collaboration: Evidence for collectivity in pp collisions at the LHC. *Phys. Lett. B* **765**, 193–220 (2017) <https://doi.org/10.1016/j.physletb.2016.12.009>
- [17] ALICE Collaboration: Multiplicity dependence of light-flavor hadron production in pp collisions at $\sqrt{s} = 7$ TeV. *Phys. Rev. C* **99**, 024906 (2019) <https://doi.org/10.1103/PhysRevC.99.024906>
- [18] ALICE Collaboration: Multiplicity dependence of π , k, and p production in pp collisions at $\sqrt{s} = 13$ tev. *Eur. Phys. J. C* **80**(8), 693 (2020) <https://doi.org/10.1140/epjc/s10052-020-8125-1>
- [19] PHENIX Collaboration: Creation of quark-gluon plasma droplets with three distinct geometries. *Nature Phys.* **15**(3), 214–220 (2019) <https://doi.org/10.1038/s41567-018-0360-0>
- [20] Nagle, J.L., Zajc, W.A.: Small System Collectivity in Relativistic Hadronic and Nuclear Collisions. *Ann. Rev. Nucl. Part. Sci.* **68**, 211–235 (2018) <https://doi.org/10.1146/annurev-nucl-101916-123209>
- [21] Cuautle, E., Paic, G.: Radial flow afterburner for event generators and the baryon puzzle. *J. Phys. G* **35**, 075103 (2008) <https://doi.org/10.1088/0954-3899/35/7/075103>
- [22] Andersson, B.: The Lund Model. Cambridge University Press, ??? (1998). <https://doi.org/10.1017/CBO9780511524363>
- [23] Andersson, B., Gustafson, G., Ingelman, G., Sjöstrand, T.: Parton Fragmentation and String Dynamics. *Phys. Rep.* **97**, 31–145 (1983) [https://doi.org/10.1016/0370-1573\(83\)90080-7](https://doi.org/10.1016/0370-1573(83)90080-7)
- [24] Bialas, A.: Fluctuations of the string tension and transverse mass distribution. *Phys. Lett. B* **466**(2), 301–304 (1999) [https://doi.org/10.1016/S0370-2693\(99\)01159-4](https://doi.org/10.1016/S0370-2693(99)01159-4)
- [25] Rosales Herrera, D., Alvarado García, J.R., Fernández Téllez, A., Ramírez, J.E., Pajares, C.: Entropy and heat capacity of the transverse momentum distribution for pp collisions at RHIC and LHC energies. *Phys. Rev. C* **109**, 034915 (2024) <https://doi.org/10.1103/PhysRevC.109.034915>
- [26] Pajares, C., Ramírez, J.E.: On the relation between the soft and hard parts of the transverse momentum distribution. *Eur. Phys. J. A* **59**(11), 250 (2023) <https://doi.org/10.1140/epja/s10050-023-01170-w>
- [27] Alvarado García, J.R., Rosales Herrera, D., Fierro, P., Ramírez, J.E., Fernández Téllez, A., Pajares, C.: Soft and hard scales of the transverse momentum distribution in the color string percolation model. *J. Phys. G Nucl. Partic.* **50**(12), 125105 (2023) <https://doi.org/10.1088/1361-6471/acfe1>
- [28] Rosales Herrera, D., Alvarado García, J.R., Fernández Téllez, A., Ramírez, J.E., Pajares, C.: Nonextensivity and temperature fluctuations of the Higgs boson production. *Phys. Rev. C* **110**(1), 015205 (2024) <https://doi.org/10.1103/PhysRevC.110.015205>
- [29] Schwinger, J.: Gauge invariance and mass. ii. *Phys. Rev.* **128**, 2425–2429 (1962) <https://doi.org/10.1103/PhysRev.128.2425>

- [30] Budini, A.A.: Generalized fluctuation relation for power-law distributions. *Phys. Rev. E* **86**, 011109 (2012) <https://doi.org/10.1103/PhysRevE.86.011109>
- [31] Budini, A.A.: Extended q -gaussian and q -exponential distributions from gamma random variables. *Phys. Rev. E* **91**, 052113 (2015) <https://doi.org/10.1103/PhysRevE.91.052113>
- [32] Collaboration, A.: Transverse momentum spectra of charged particles in proton-proton collisions at $\sqrt{s} = 900$ GeV with ALICE at the LHC. *Phys. Lett. B* **693**, 53–68 (2010) <https://doi.org/10.1016/j.physletb.2010.08.026>
- [33] ALICE Collaboration: Transverse momentum spectra and nuclear modification factors of charged particles in pp, p-Pb and Pb-Pb collisions at the LHC. *JHEP* **11**, 013 (2018) [https://doi.org/10.1007/JHEP11\(2018\)013](https://doi.org/10.1007/JHEP11(2018)013)
- [34] ALICE Collaboration: Transverse momentum spectra and nuclear modification factors of charged particles in Xe-Xe collisions at $\sqrt{s_{NN}} = 5.44$ TeV. *Phys. Lett. B* **788**, 166–179 (2019) <https://doi.org/10.1016/j.physletb.2018.10.052>
- [35] ALICE Collaboration: Charged-particle production as a function of multiplicity and transverse sphericity in pp collisions at $\sqrt{s} = 5.02$ and 13 TeV. *Eur. Phys. J. C* **79**(10), 857 (2019) <https://doi.org/10.1140/epjc/s10052-019-7350-y>
- [36] ALICE Collaboration: Multiplicity dependence of charged-particle production in pp, p-Pb, Xe-Xe and Pb-Pb collisions at the LHC. *Phys. Lett. B* **845**, 138110 (2023) <https://doi.org/10.1016/j.physletb.2023.138110>
- [37] Bjorken, J.D. Technical Report FERMILAB-PUB-82-059-THY (August 1982)
- [38] PHENIX Collaboration: Suppression of hadrons with large transverse momentum in central Au+Au collisions at $\sqrt{s_{NN}} = 130$ -GeV. *Phys. Rev. Lett.* **88**, 022301 (2002) <https://doi.org/10.1103/PhysRevLett.88.022301>
- [39] STAR Collaboration: Centrality dependence of high p_T hadron suppression in Au+Au collisions at $\sqrt{s_{NN}} = 130$ -GeV. *Phys. Rev. Lett.* **89**, 202301 (2002) <https://doi.org/10.1103/PhysRevLett.89.202301>
- [40] Bjorken, J.D.: Highly Relativistic Nucleus-Nucleus Collisions: The Central Rapidity Region. *Phys. Rev. D* **27**, 140–151 (1983) <https://doi.org/10.1103/PhysRevD.27.140>
- [41] STAR Collaboration: Systematic Measurements of Identified Particle Spectra in pp , d^+ Au and Au+Au Collisions from STAR. *Phys. Rev. C* **79**, 034909 (2009) <https://doi.org/10.1103/PhysRevC.79.034909>
- [42] Feal, X., Pajares, C., Vazquez, R.A.: Thermal behavior and entanglement in Pb-Pb and p - p collisions. *Phys. Rev. C* **99**(1), 015205 (2019) <https://doi.org/10.1103/PhysRevC.99.015205>
- [43] CMS Collaboration: Observation of Long-Range Near-Side Angular Correlations in Proton-Proton Collisions at the LHC. *JHEP* **09**, 091 (2010) [https://doi.org/10.1007/JHEP09\(2010\)091](https://doi.org/10.1007/JHEP09(2010)091)
- [44] ALICE Collaboration: Production of light nuclei and anti-nuclei in pp and pb-pb collisions at energies available at the cern large hadron collider. *Phys. Rev. C* **93**, 024917 (2016) <https://doi.org/10.1103/PhysRevC.93.024917>
- [45] Kalaydzhyan, T., Shuryak, E.: Collective flow in high-multiplicity proton-proton collisions. *Phys. Rev. C* **91**, 054913 (2015) <https://doi.org/10.1103/PhysRevC.91.054913>